

# Difference in proton radii of mirror nuclei as a possible surrogate for the neutron skin

Junjie Yang and J. Piekarewicz

*Department of Physics, Florida State University, Tallahassee, FL 32306, USA*

(Dated: November 20, 2021)

It has been recently suggested that differences in the charge radii of mirror nuclei are proportional to the neutron-skin thickness of neutron-rich nuclei and to the slope of the symmetry energy  $L$  [B.A. Brown Phys. Rev. Lett. 119, 122502 (2017)]. The determination of the neutron skin has important implications for nuclear physics and astrophysics. Although the use of electroweak probes provides a largely model-independent determination of the neutron skin, the experimental challenges are enormous. Thus, the possibility that differences in the charge radii of mirror nuclei may be used as a surrogate for the neutron skin is a welcome alternative. To test the validity of this assumption we perform calculations based on a set of relativistic energy density functionals that span a wide region of values of  $L$ . Our results confirm that the difference in charge radii of various neutron-deficient nickel isotopes and their corresponding mirror nuclei is indeed strongly correlated to both the neutron-skin thickness and  $L$ . Moreover, given that various neutron-star properties are also sensitive to  $L$ , a data-to-data relation emerges between the difference in charge radii of mirror nuclei and the radius of low-mass neutron stars.

PACS numbers: 21.10.Gv, 21.60.Jz, 21.65.Ef, 26.60.Kp

The neutron-rich skin of medium and heavy nuclei is a fundamental nuclear property that has gained prominence almost two decades ago because of its strong correlation to the equation of state of neutron-rich matter, primarily to the slope of the symmetry energy  $L$  [1–4]. Given that the weak charge of the neutron is significantly larger than the corresponding one for the proton, parity-violating electron scattering offers a clean probe of neutron densities that is free from strong-interaction uncertainties [5]. The pioneering Lead Radius Experiment (PREX) at the Jefferson Laboratory has provided the first model-independent evidence on the existence of a neutron-rich skin in  $^{208}\text{Pb}$  [6, 7]. In the near future a follow-up experiment (PREX-II) is envisioned to reach the desired 0.06 fm sensitivity in the neutron radius of  $^{208}\text{Pb}$  and a brand new experiment on  $^{48}\text{Ca}$  promises to bridge the gap between modern ab initio approaches and density functional theory [8]. Moreover, the study of neutron-rich matter with unusual features such as large neutron skins is one of the key science drivers for the Facility for Rare Isotope Beams (FRIB) [9, 10].

Besides being of fundamental importance in nuclear structure, the neutron-rich skin of medium to heavy nuclei plays a critical role in the determination of the equation of state (EOS) of neutron-rich matter. In turn, important dynamical signatures observed in the collision of heavy ions are encoded in the EOS [11–18]. Further, despite a difference in length scales of 18 orders of magnitude, the neutron-skin thickness of  $^{208}\text{Pb}$  and the radius of a neutron star share a common dynamical origin [19–25]. Indeed, the only input that the structure of spherically symmetric neutron stars is sensitive to is the equation of state of neutron-rich matter. This fact alone has created a unique synergy between nuclear physics and astrophysics.

Although there is little doubt that parity violating elec-

tron scattering provides the cleanest probe of neutron densities, the experimental challenges associated with such experiments are enormous. This fact has motivated searches for complementary observables to the neutron skin that also display a strong sensitivity to the density dependence of the symmetry energy. Particularly valuable was the identification of the electric dipole polarizability ( $\alpha_{\text{D}}$ ) as a strong isovector indicator [26]. The electric dipole polarizability encodes the response of the nucleus to an externally applied electric field and is directly proportional to the *inverse* energy weighted sum of the isovector dipole response [27]. The isovector dipole resonance is commonly identified as an out-of-phase oscillation of protons against neutrons, with the symmetry energy acting as the restoring force. Since  $\alpha_{\text{D}}$  was first identified as a strong isovector indicator, a flurry of activity ensued in both theoretical [28–34] and experimental fronts [35–42].

In the ongoing quest to determine the equation of state of neutron-rich matter, B.A. Brown has recently identified a physical observable that is closely related to the neutron skin [43]. The argument is both simple and elegant: in the limit of exact charge symmetry, the neutron radius of a given nucleus is identical to the proton radius of its mirror nucleus. That is,

$$R_{\text{skin}}(Z, N) \equiv R_n(Z, N) - R_p(Z, N) \\ \stackrel{\text{c.s.}}{=} R_p(N, Z) - R_p(Z, N) \equiv R_{\text{mirr}}(Z, N). \quad (1)$$

For example, in the case of  $^{48}\text{Ca}$  [8]:

$$R_{\text{skin}}(^{48}\text{Ca}) \stackrel{\text{c.s.}}{=} R_p(^{48}\text{Ni}) - R_p(^{48}\text{Ca}) \equiv R_{\text{mirr}}^{48}. \quad (2)$$

While the basic idea is appealing, the ultimate test of its validity relies on its robustness against the all-important Coulomb corrections. Indeed, most of the work in Ref. [43] was devoted to show that the differences in the charge radii of mirror nuclei as predicted by

a set of Skyrme functionals is proportional to the slope of the symmetry energy at saturation density—even in the presence of Coulomb corrections. In this work we show that those findings remain valid in the relativistic approach. Moreover, we also show how  $R_{\text{mirr}}$ , just as  $R_{\text{skin}}$ , is correlated to the radius of low-mass neutron stars, a stellar property that is highly sensitive to the density dependence of the symmetry energy.

In the relativistic mean field (RMF) approach pioneered by Serot and Walecka [44, 45], the basic fermionic constituents are protons and neutrons interacting via photon exchange as well as through the exchange of various mesons of distinct Lorentz and isospin character. Besides the conventional Yukawa couplings of the mesons to the relevant nuclear currents, the model is supplemented by several nonlinear meson coupling that are essential for its ultimate success [19, 46, 47]. Besides a progressive increase in the complexity of the model, sophisticated fitting protocols are now used for its calibration. Indeed, properties of finite nuclei, their monopole response, and even a few properties of neutron stars now provide critical inputs in the determination of the relativistic functional [25].

To explore some of the interesting correlations that emerged in Ref. [43], but now in the relativistic context, we employ a set of 14 energy density functionals that span a wide region of values of the slope parameter:  $L \simeq 50\text{--}140$  MeV. In turn, this corresponds to a neutron-skin thickness in  $^{208}\text{Pb}$  ranging from about  $R_{\text{skin}}^{208} \simeq 0.15$  to 0.33 fm, well within the limits of the PREX measurement [6, 7]. Parameter sets for the models adopted in this contribution are: NL3 [48, 49], FSUGold [50], IU-FSU [51], TAMUC-FSU [52], FSUGold2 [25], and FSUGarnet [53]. Although most of these models have been accurately calibrated, a few of them were obtained by systematically varying their two isovector parameters, while leaving the isoscalar sector intact. This enables one to modify the poorly constrained density dependence of the symmetry energy without compromising the success of the model in the isoscalar sector. In essence, all these models reproduce nuclear observables near stability, yet may vary widely in their predictions for the properties of exotic nuclei far from stability.

In Fig. 1(a) we display data-to-data relations between the neutron-skin thickness of  $^{48}\text{Ca}$  and the difference in proton radii between three neutron-deficient nickel isotopes and their corresponding mirror nuclei; the same information is shown in Fig. 1(b) but now for  $^{208}\text{Pb}$ . For example, the blue circles denote the difference in proton radii in the  $A = 50$  sector:  $R_{\text{mirr}}^{50} \equiv R_p(^{50}\text{Ni}) - R_p(^{50}\text{Ti})$ . Besides computing proton radii along the  $A = 50, 52, 54$  isobars, we tried to calculate the proton radius of  $^{48}\text{Ni}$  but were unable to bind the  $f^{7/2}$  protons—especially in RMF models having a soft symmetry energy. As indicated by the correlation coefficients displayed in parentheses in Fig. 1, there is a strong correlation between  $R_{\text{skin}}$  and  $R_{\text{mirr}}$  for both  $^{48}\text{Ca}$  and  $^{208}\text{Pb}$ , at least for the representative set of models used in this work. Also

shown are the linear regression slopes obtained from the statistical analysis. Clearly, the larger the value of the slope the more accurate the determination of the charge radius of the *unstable* neutron-deficient nickel isotope needs to be. Indeed, if one is interested in the determination of the neutron skin of  $^{48}\text{Ca}$  to a precision of 0.02 fm [8], then one must measure the charge radius of  $^{54}\text{Ni}$  to better than 0.004 fm; note that the charge radius of its *stable* mirror nucleus  $^{54}\text{Fe}$  is already known to 0.002 fm [54]. On the other hand, for the  $A = 50$  case the charge radius of  $^{50}\text{Ni}$  needs to be determined to “only” 0.012 fm. However, in this case the experimental challenge is formidable, as  $^{58}\text{Ni}$  is the most neutron-deficient isotope with a well measured charge radius [54]. Yet, we are confident that with the commissioning of new and more intense radioactive beam facilities, the experimental community will continue to rise up to the challenge. Note that while the regression slopes almost double for  $^{208}\text{Pb}$ , the aim of the PREX-II experiment is to determine the neutron radius of  $^{208}\text{Pb}$  to 0.06 fm. However, we caution against a possible model dependence of our results, as the correlation between the neutron skin of  $^{208}\text{Pb}$  and that of  $^{48}\text{Ca}$  does not appear to be as strong as suggested here; see for example Fig. 2(b) of Ref. [29].

Having established the existence of a strong correlation between  $R_{\text{skin}}$  and  $R_{\text{mirr}}$ , we now proceed to explore the sensitivity of the latter to the slope of the symmetry energy. Recall that the slope of the symmetry energy is defined as

$$L = \left( 3\rho \frac{\partial \mathcal{S}}{\partial \rho} \right)_{\rho=\rho_0}, \quad (3)$$

where  $\mathcal{S}(\rho)$  is the symmetry energy, namely, the energy cost of turning neutrons into protons (or vice versa) in symmetric nuclear matter.

In Fig. 2(a) we plot the difference in the proton radii of mirror nuclei as a function of  $L$ . The observed correlation is as strong as the one between the neutron-skin thickness of  $^{48}\text{Ca}$  and  $L$  (figure not shown). While this suggests an efficient tool to constrain a fundamental parameter of the equation of state, the robustness of this result should be tested against a possible model dependency. Clearly, it would be ideal to extend this approach to the heavy-mass region where the surface to volume ratio is more favorable, as in the case of  $^{208}\text{Pb}$  whose neutron skin has been firmly established as a proxy for  $L$ . Unfortunately, exploiting the isovector character of mirror nuclei is limited to a fairly narrow region of the nuclear chart.

Shown in Fig. 2(b) is a similar plot but now against the slope of the symmetry energy at the slightly lower density of  $\tilde{\rho}_0 = 0.10$  fm $^{-3}$ , or about 2/3 of the density at saturation. Note that  $\tilde{L}$  is defined exactly as in Eq. (3) but now evaluated at  $\rho = \tilde{\rho}_0$ . In all three cases the correlation becomes tighter. That a lower density than saturation represents a better choice to determine the symmetry energy has been emphasized repeatedly; see for example Refs. [1, 2, 18–20, 55–58]. Indeed, given that so far the

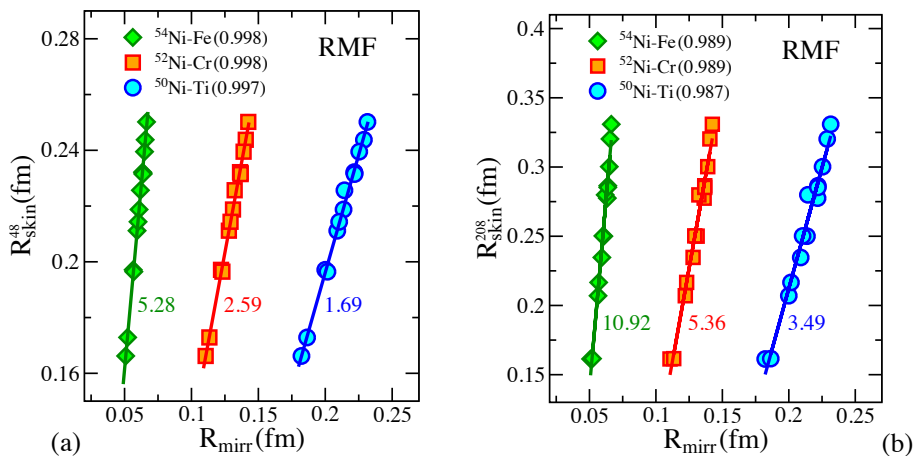


FIG. 1: (Color online) (a) Data-to-data relations between the neutron-skin thickness of  $^{48}\text{Ca}$  and the difference in proton radii between a few neutron-deficient nickel isotopes and their corresponding mirror nuclei along the  $A=50, 52, 54$  isobars. Numbers in parentheses represent the correlation coefficients and the numbers next to the lines the linear regression slopes. (b) Same but now for the neutron-skin thickness of  $^{208}\text{Pb}$ .

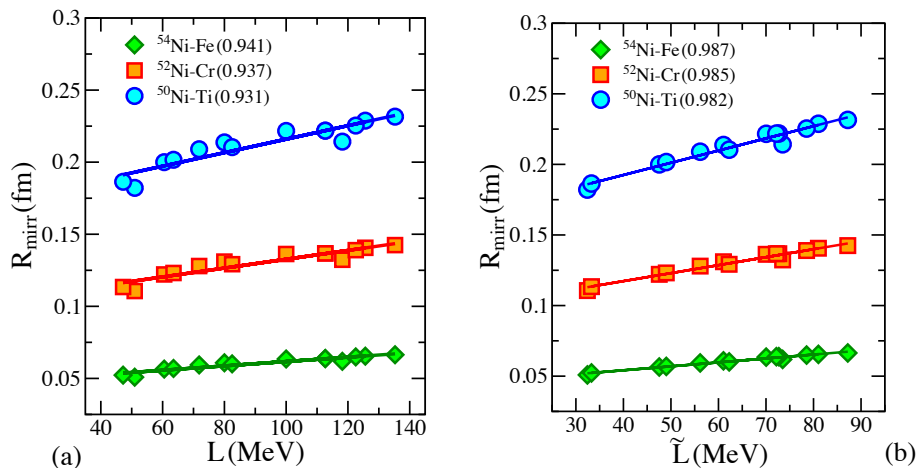


FIG. 2: (Color online) (a) Difference in proton radii along the  $A=50, 52, 54$  isobars as a function of the slope of the symmetry energy at saturation density. Numbers in parentheses represent the correlation coefficients. (b) Same but now as a function of the slope of the symmetry energy at the lower density of  $0.10\text{ fm}$ .

isovector sector is largely informed by the binding energy of stable neutron-rich nuclei, the symmetry energy is better constrained at a density that results from an average of the nuclear interior and the nuclear surface.

We finish this contribution by exploring a possible connection between  $R_{\text{mirr}}^{50} \equiv R_p(^{50}\text{Ni}) - R_p(^{50}\text{Ti})$  and the radius of a neutron star, a stellar property that is known to be particularly sensitive to the density dependence of the symmetry energy [59]. Note that an intriguing correlation exists that involves objects that differ in size by 18 orders of magnitude: the smaller the neutron-skin thickness of  $^{208}\text{Pb}$  the smaller the size of the neutron star [20]. That is, whether pushing against surface tension in  $^{208}\text{Pb}$  or against gravity in a “low-mass” neutron star [21], it is the pressure of neutron-rich matter around saturation density that determines both the thickness of the neu-

tron skin and the radius of a neutron star. Given the strong correlation between  $R_{\text{skin}}^{208}$  and  $R_{\text{mirr}}^{50}$  displayed in Fig. 1b, we find natural to explore a possible connection between the latter and the stellar radius. Thus, we display in Fig. 3 neutron-star radii as a function of  $R_{\text{mirr}}^{50}$  for neutron stars with masses of  $M_\star = 0.8, 1.0, 1.2, 1.4 M_\odot$ . We observe a strong correlation—with a correlation coefficient of  $r = 0.96$ —between  $R_{\text{mirr}}^{50}$  and the radius of a  $M_\star = 0.8 M_\odot$  neutron star. The correlation is strong because for such a relatively light neutron star, the central density remains well below twice nuclear-matter saturation density even for the softest of the RMF models. However, the correlation weakens with increasing stellar mass because the radius becomes sensitive to the pressure at densities significantly higher than those probed in the laboratory. For example, in the case of a  $M_\star = 1.4 M_\odot$

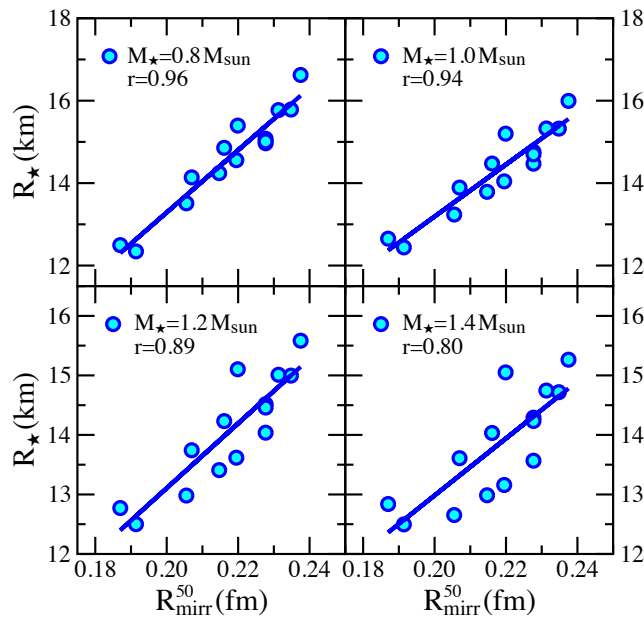


FIG. 3: (Color online) Stellar radii for neutron stars with masses of  $M_* = 0.8, 1.0, 1.2, 1.4 M_\odot$  as a function of the difference in proton radii between  $^{50}\text{Ni}$  and  $^{50}\text{Ti}$ . Here  $r$  is the correlation coefficient deduced from a linear regression.

the correlation weakens to  $r = 0.8$  because now the density in the stellar core exceeds three times nuclear matter saturation density. As in the case of the neutron-skin thickness of  $^{208}\text{Pb}$ , we conclude that it may be possible to infer some fundamental properties of low-mass neutron stars from the structure of atomic nuclei.

In summary, inspired by the simple and elegant idea presented in Ref. [43] that suggests that differences in the charge radii of mirror nuclei are correlated to both the neutron-skin thickness of neutron-rich nuclei and the slope of the symmetry energy, we have investigated the validity of these correlations in the relativistic framework. Using a set of accurately calibrated relativistic energy density functionals that span a wide range of values for the slope of the symmetry energy  $L$ , we have confirmed the results of Ref. [43]. Moreover, we have extended our results to the neutron-star domain and reported a strong

correlation between the difference in the proton radii between  $^{50}\text{Ni}$  and  $^{50}\text{Ti}$ , and the radii of low-mass neutron stars. Thus, at least within the context of the RMF models employed in this work, we have established that the difference in charge radii may serve as a credible surrogate for the neutron-skin of neutron-rich nuclei. Moreover, we concluded that accurate measurements of the charge radii of neutron deficient nickel isotopes may have important implications for the structure of low-mass neutron stars.

The realization that the neutron-skin thickness of neutron-rich nuclei could have such a dramatic impact in areas far beyond the nuclear-structure domain has created a flurry of activity that continues until today. We trust that the ideas introduced in Ref. [43] and expanded in this presentation will also stimulate considerable experimental and theoretical activity. Theoretically, both ab initio models and energy density functionals of increasing sophistication are in an excellent position to predict with quantifiable uncertainties the charge distribution of neutron-deficient nuclei. Experimentally, enormous technical advances have resulted in pioneering measurements of the charge radii of unstable neutron-rich isotopes at such facilities as ISOLDE-CERN [60] and soon at RIKEN-SCRIT [61]. We are confident that these techniques may also be used to measure the charge radius of the neutron-deficient isotopes discussed in this work. Moreover, such remarkable level of activity will only increase with the commissioning of new radioactive beam facilities throughout the world. As we enter a golden era in nuclear structure that will see a paradigm shift in fundamental core concepts, we are confident that “unprecedented access to a vast new array of nuclei will result in scientific breakthroughs and major advances in our understanding of nuclei and their role in the cosmos” [10].

### Acknowledgments

This material is based upon work supported by the U.S. Department of Energy Office of Science, Office of Nuclear Physics under Award Number DE-FG02-92ER40750.

- 
- [1] B. A. Brown, Phys. Rev. Lett. **85**, 5296 (2000).
  - [2] R. J. Furnstahl, Nucl. Phys. **A706**, 85 (2002).
  - [3] M. Centelles, X. Roca-Maza, X. Viñas, and M. Warda, Phys. Rev. Lett. **102**, 122502 (2009).
  - [4] X. Roca-Maza, M. Centelles, X. Viñas, and M. Warda, Phys. Rev. Lett. **106**, 252501 (2011).
  - [5] T. Donnelly, J. Dubach, and I. Sick, Nucl. Phys. **A503**, 589 (1989).
  - [6] S. Abrahamyan, Z. Ahmed, H. Albatineh, K. Aniol, D. S. Armstrong, et al., Phys. Rev. Lett. **108**, 112502 (2012).
  - [7] C. J. Horowitz, Z. Ahmed, C. M. Jen, A. Rakhman, P. A. Souder, et al., Phys. Rev. **C85**, 032501 (2012).
  - [8] J. Mammei et al., *CREX: Parity-violating measurement of the weak-charge distribution of  $^{48}\text{Ca}$  to 0.02 fm accuracy* (2013), URL <http://hallaweb.jlab.org/parity/prex/c-rex/c-rex.pdf>.
  - [9] A. B. Balantekin et al., Mod. Phys. Lett. **A29**, 1430010 (2014).
  - [10] *Reaching for the Horizon; The 2015 Long Range Plan for Nuclear Science* (2015).
  - [11] M. B. Tsang et al., Phys. Rev. Lett. **92**, 062701 (2004).

- [12] L.-W. Chen, C. M. Ko, and B.-A. Li, Phys. Rev. Lett. **94**, 032701 (2005).
- [13] A. W. Steiner and B.-A. Li, Phys. Rev. **C72**, 041601 (2005).
- [14] D. V. Shetty, S. J. Yennello, and G. A. Souliotis, Phys. Rev. **C76**, 024606 (2007).
- [15] M. B. Tsang et al., Phys. Rev. Lett. **102**, 122701 (2009).
- [16] B.-A. Li, L.-W. Chen, and C. M. Ko, Phys. Rept. **464**, 113 (2008).
- [17] M. Tsang, J. Stone, F. Camera, P. Danielewicz, S. Gandolfi, et al., Phys. Rev. **C86**, 015803 (2012).
- [18] C. J. Horowitz, E. F. Brown, Y. Kim, W. G. Lynch, R. Michaels, et al., J. Phys. **G41**, 093001 (2014).
- [19] C. J. Horowitz and J. Piekarewicz, Phys. Rev. Lett. **86**, 5647 (2001).
- [20] C. J. Horowitz and J. Piekarewicz, Phys. Rev. **C64**, 062802 (2001).
- [21] J. Carriere, C. J. Horowitz, and J. Piekarewicz, Astrophys. J. **593**, 463 (2003).
- [22] A. W. Steiner, M. Prakash, J. M. Lattimer, and P. J. Ellis, Phys. Rept. **411**, 325 (2005).
- [23] B.-A. Li and A. W. Steiner, Phys. Lett. **B642**, 436 (2006).
- [24] J. Erler, C. J. Horowitz, W. Nazarewicz, M. Rafalski, and P.-G. Reinhard, Phys. Rev. **C87**, 044320 (2013).
- [25] W.-C. Chen and J. Piekarewicz, Phys. Rev. **C90**, 044305 (2014).
- [26] P.-G. Reinhard and W. Nazarewicz, Phys. Rev. **C81**, 051303 (2010).
- [27] M. N. Harakeh and A. van der Woude, *Giant Resonances-Fundamental High-frequency Modes of Nuclear Excitation* (Clarendon, Oxford, 2001).
- [28] J. Piekarewicz, Phys. Rev. **C83**, 034319 (2011).
- [29] J. Piekarewicz, B. Agrawal, G. Colò, W. Nazarewicz, N. Paar, et al., Phys. Rev. **C85**, 041302(R) (2012).
- [30] P. Reinhard and W. Nazarewicz, Phys. Rev. **C87**, 014324 (2013).
- [31] X. Roca-Maza, M. Centelles, X. Viñas, M. Brenna, G. Colò, et al., Phys. Rev. **C88**, 024316 (2013).
- [32] X. Roca-Maza, X. Viñas, M. Centelles, B. K. Agrawal, G. Colò, N. Paar, J. Piekarewicz, and D. Vretenar, Phys. Rev. **C92**, 064304 (2015).
- [33] G. Hagen et al., Nature Phys. (2015).
- [34] J. Piekarewicz, Phys. Rev. **C73**, 044325 (2006).
- [35] A. Tamii et al., Phys. Rev. Lett. **107**, 062502 (2011).
- [36] I. Poltoratska, P. von Neumann-Cosel, A. Tamii, T. Adachi, C. Bertulani, et al., Phys. Rev. **C85**, 041304 (2012).
- [37] A. Tamii, P. von Neumann-Cosel, and I. Poltoratska, Eur. Phys. J. **A50**, 28 (2014).
- [38] D. Savran, T. Aumann, and A. Zilges, Prog. Part. Nucl. Phys. **70**, 210 (2013).
- [39] T. Hashimoto et al., Phys. Rev. **C92**, 031305 (2015).
- [40] D. Rossi, P. Adrich, F. Aksouh, H. Alvarez-Pol, T. Aumann, et al., Phys. Rev. Lett. **111**, 242503 (2013).
- [41] J. Birkhan et al., Phys. Rev. Lett. **118**, 252501 (2017).
- [42] A. P. Tonchev et al., Phys. Lett. **B773**, 20 (2017).
- [43] B. A. Brown, Phys. Rev. Lett. **119**, 122502 (2017).
- [44] J. D. Walecka, Annals Phys. **83**, 491 (1974).
- [45] B. D. Serot and J. D. Walecka, Adv. Nucl. Phys. **16**, 1 (1986).
- [46] J. Boguta and A. R. Bodmer, Nucl. Phys. **A292**, 413 (1977).
- [47] H. Mueller and B. D. Serot, Nucl. Phys. **A606**, 508 (1996).
- [48] G. A. Lalazissis, J. König, and P. Ring, Phys. Rev. **C55**, 540 (1997).
- [49] G. A. Lalazissis, S. Raman, and P. Ring, At. Data Nucl. Data Tables **71**, 1 (1999).
- [50] B. G. Todd-Rutel and J. Piekarewicz, Phys. Rev. Lett. **95**, 122501 (2005).
- [51] F. J. Fattoyev, C. J. Horowitz, J. Piekarewicz, and G. Shen, Phys. Rev. **C82**, 055803 (2010).
- [52] F. Fattoyev and J. Piekarewicz, Phys. Rev. Lett. **111**, 162501 (2013).
- [53] W.-C. Chen and J. Piekarewicz, Phys. Lett. **B748**, 284 (2015).
- [54] I. Angeli and K. Marinova, At. Data Nucl. Data Tables **99**, 69 (2013).
- [55] M. Farine, J. Pearson, and B. Rouben, Nucl. Phys. A **304**, 317 (1978).
- [56] C. Ducoin, J. Margueron, C. Providencia, and I. Vidana, Phys. Rev. **C83**, 045810 (2011).
- [57] Z. Zhang and L.-W. Chen, Phys. Lett. **B726**, 234 (2013).
- [58] B. A. Brown, Phys. Rev. Lett. **111**, 232502 (2013).
- [59] J. M. Lattimer and M. Prakash, Phys. Rept. **442**, 109 (2007).
- [60] R. F. Garcia Ruiz et al., Nature Phys. **12**, 594 (2016).
- [61] K. Tsukada et al., Phys. Rev. Lett. **118**, 262501 (2017).